

Closed-form Throughput Expressions for CSMA Networks with Collisions and Hidden Terminals

Bruno Nardelli and Edward W. Knightly
ECE Department, Rice University, Houston, TX
Technical Report TREE1107

Abstract—We present a novel modeling approach to derive closed-form throughput expressions for CSMA networks with hidden terminals. The key modeling principle is to break the interdependence of events in a wireless network using conditional expressions that capture the effect of a specific factor each, yet preserve the required dependences when combined together. Different from existing models that use numerical aggregation techniques, our approach is the first to jointly characterize the three main critical factors affecting flow throughput (referred to as hidden terminals, information asymmetry and flow-in-the-middle) within a single analytical expression. We have developed a symbolic implementation of the model, that we use for validation against realistic simulations and experiments with real wireless hardware, observing high model accuracy in all evaluated scenarios. The derived closed-form expressions enable new analytical studies of capacity and protocol performance that would not be possible with prior models. We illustrate this through an application of network utility maximization in complex networks with collisions, hidden terminals, asymmetric interference and channel errors. Despite that such problematic scenarios make utility maximization a challenging problem, the model-based optimization yields vast fairness gains and an average per-flow throughput gain higher than 500% with respect to 802.11 in the evaluated networks.

I. INTRODUCTION

From the beginnings of research on CSMA wireless networks, significant effort has been devoted to devise analytical expressions of protocol performance, with pioneering work such as [1]. Although [1] is specific to fully-connected networks, where all terminals are in transmission range of each other, it established a first relation between system parameters (such as offered load) and attainable throughput, providing an important contribution to understanding CSMA protocols.

Subsequent work focused on modeling CSMA performance in more general wireless networks, where not all the nodes are in transmission range of each other. In such networks, multiple factors contribute to determine the flow throughput distribution. For example, *hidden terminals* are known to increase the probability of packet collisions, which can drastically reduce throughput [17]. Also, the relative position of nodes in a topology can yield a high probability of collision at one receiver but a high success rate in another one. Such a configuration, termed “*Information Asymmetry*” in [10], can result in large throughput disparities among flows. In addition, signals from hidden transmitters can overlap in time leaving no silent periods for other nodes to transmit, as in topologies with a “*Flow-In-the-Middle*” [14], [19]. Such coordination problems can significantly alter the throughput distribution, or even induce complete starvation of specific network flows.

In wireless CSMA networks, many of these factors can manifest simultaneously, which makes system modeling a daunting task. State-of-the-art wireless CSMA models, such as [11]–[15], face this problem by the use of a two-step approach. First, they separately model each factor with a specific analytical expression, decoupling them from the rest of the network. Second, they combine the obtained results using iterative procedures to determine the throughput distribution at the network scale. Despite the undeniable importance of these works, the iterative phase is only suitable for numerical computations, and therefore cannot provide closed-form expressions for network throughput analysis.

In this work, we present closed-form expressions of throughput for CSMA networks with collisions and hidden terminals. While hidden terminals are not the only factor affecting flow throughput in CSMA wireless networks, our method is general enough to capture the three aforementioned topological factors (namely hidden terminals, information asymmetry and flow-in-the-middle), identified by previous work as critical to determine the flow throughput distribution at the network scale [10], [14]. In contrast with existing models, our approach does not rely on any numerical aggregation method. Indeed, it is the first model characterizing the joint effect of all such critical factors within a single closed-form analytical expression.

The key modeling principle to incorporate the effect of multiple factors into a single equation is to break the interdependence of events using conditional expressions, which capture the effect of a single factor each, yet preserve the required dependences when combined together into a larger expression. As a result, the model is modular and easy to extend to incorporate additional factors affecting flow throughput adding appropriate expressions to capture their effects. In addition, it is based on simple, standard modeling techniques which makes it easy to adopt for a wide-range of network analysis applications.

While we use a highly simplified channel model as in [1], [2], [9], [14], unlike [1], [6] we do not require full connectivity, and unlike [7], [9], we support asymmetric interference and partially-overlapping transmissions. Furthermore, our experimental validation shows that, despite the simplifications, the model features play an essential role in characterizing CSMA protocol performance, yielding high accuracy in realistic wireless scenarios (with less than 2% normalized error averaged over all evaluated data points).

The derived expressions enable unprecedented studies of

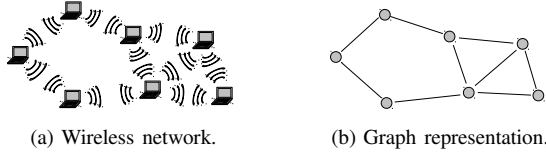


Fig. 1: A wireless network and its graph representation.

capacity and protocol performance in networks with hidden terminals, asymmetries, collisions and channel errors. As a concrete example, we show how the model can be used to determine per-node contention window assignments that maximize throughput-based utility in such networks. While the problematic scenarios considered here make utility maximization a very hard problem, the proposed method yields excellent results, preventing starvation of disadvantaged flows and attaining an average per-flow throughput gain of more than 500% with respect to 802.11 in the evaluated networks.

This document is organized as follows. Section II introduces the analytical framework and derives the proposed model. Section III validates the model by means of simulations and experiments. Section IV demonstrates the use of the derived expressions applied to network utility maximization. Section V discusses related work and finally, Section VI concludes.

II. ANALYTICAL MODEL

A. CSMA wireless network

We represent a wireless network with a graph $G = (\mathcal{V}, \mathcal{E})$ where \mathcal{V} is the set of nodes and $\mathcal{E} \subseteq \mathcal{V}^2$ is the set of links, i.e., $(u, v) \in \mathcal{E}$ belongs to \mathcal{E} iff u and v are in transmission range of each other (e.g., see Fig 1).¹ A subset \mathcal{F} of the node pairs in \mathcal{E} denotes the set of flows in the network. Given $f = (i, j) \in \mathcal{F}$, the node i is the *transmitter* (or the *source*) of flow f , and node j is the *receiver* (or *destination*) of flow f .²

All nodes use single antennas operating on the same channel. Hence, simultaneous signals overlapping at a receiver collide and cannot be decoded. Also, the same node can operate either as a transmitter or a receiver, alternating between the two roles, but it cannot transmit and receive at the same time. To account for these two cases, we say that flow $f = (u, v)$ *interferes* with flow $g = (i, j)$ if either $(u, j) \in \mathcal{E}$ or $u = j$.³ Then, we denote as $\mathcal{I}(g)$ the set of flows interfering with g , i.e., $\mathcal{I}(g) = \{(u, v) \in \mathcal{F} / (u, j) \in \mathcal{E} \text{ or } u = j\}$.

Nodes execute a CSMA protocol analogous to 802.11 such that, before transmitting, node u senses the channel to verify that no neighboring transmitters are active. If the channel is *idle*, u initializes an integer variable termed the *back-off counter* to a random value uniformly distributed within a *contention window (CW)*. Time is divided into short *time slots*, and transmitter u starts a countdown procedure, decrementing the back-off counter by 1 at the end of each time slot during

which the channel remained idle. When the back-off counter reaches zero, u starts a transmission of fixed duration d . Whenever node u senses the channel *busy* it interrupts any countdown procedure and defers its transmission. Once the ongoing transmissions complete and the channel is sensed free again, u re-initializes its back-off counter and begins a new countdown procedure (we assume fully-backlogged flows, i.e., a flow source always has a packet available to transmit).

Even with *carrier sensing (CS)*, simultaneous transmissions at interfering flows are possible. First, propagation delays can prevent two neighbor transmitters from sensing each other if they decide to transmit at the same time slot. Second, transmitters out of transmission range are unable to sense each other's transmissions, drastically increasing the collision probability. To treat these two cases separately, we divide the set $\mathcal{I}(f)$ of flows interfering with $f = (u, v) \in \mathcal{F}$ into two disjoint subsets as follows. Denote as $\mathcal{I}_r(f)$ the set of flows in $\mathcal{I}(f)$ whose transmitters are in transmission range of u , i.e., $\mathcal{I}_r(f) = \{(i, j) \in \mathcal{I}(f) / (u, i) \in \mathcal{E}\}$. Similarly, denote as $\mathcal{I}_h(f)$ the set of flows in $\mathcal{I}(f)$ whose transmitters are out of the transmission range of u , i.e., $\mathcal{I}_h(f) = \{(i, j) \in \mathcal{I}(f) / (u, i) \notin \mathcal{E}\}$.

Typical CSMA implementations use adaptive mechanisms, such as *Binary Exponential Back-off (BEB)*, to regulate the CW size. In this work, we do not assume nor require any specific mechanism controlling the CW size of nodes. Rather, we address the more fundamental problem of understanding the relation between CW sizes and flow throughput regardless of *how* such CW sizes are chosen. Thus, our approach is general, and can be applied to the design and evaluation of either static or adaptive CSMA protocols as long as the mean back-off time for each node is known.

B. General analytical framework

The key to accurately determine each flow's service rate is to account for both the fraction of a flow's transmission time and the probability of success for such transmissions. In our analytical framework, we account for these two quantities by expressing the throughput of a flow f as the product

$$\gamma_f = T(f) \times S(f) \quad (1)$$

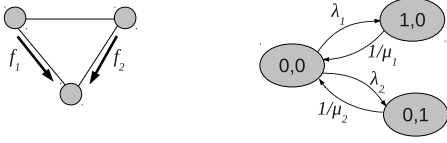
where γ_f is the long-term average throughput received by flow f , $T(f)$ is the fraction of transmission time by f 's source and $S(f)$ is the conditional probability that a packet of flow f is successfully received given that it is transmitted.

The fraction of transmission time $T(\cdot)$ can be derived for flows in an arbitrary topology using the *continuous-time CSMA model* due to [5]. In such a model, the back-off time and transmission duration of a flow f are assumed to be exponentially distributed, with means $1/\lambda_f$ and μ_f , respectively. Then, the network dynamics can be captured by a continuous-time reversible Markov chain M , where each state describes the set of active flows in the network. More precisely, for each state $m \in M$, the value $m_f \in \{0, 1\}$ indicates whether flow f is

¹As it will be discussed later, links need not be perfect and the model admits specifying channel error rates in a per-link manner.

²Thus, each element in \mathcal{F} is an *ordered pair* denoting an *unidirectional flow*. *Bidirectional* flows may be represented including in \mathcal{F} two node pairs in reverse order.

³Note that this definition of interference is general enough to admit *asymmetric* interference relations among flows.



(a) Graph representation of a two-flow wireless network. (b) Markov chain model of the same network.

Fig. 2: A two-flow wireless network with transmitters in transmission range of each other, and its Markov chain model.

active (see Fig. 2 for an example).⁴

The stationary distribution π of such Markov chain has the known closed-form

$$\forall m \in M, \quad \pi_m = \frac{\prod_{f:m_f=1} \lambda_f \mu_f}{\sum_{n \in M} \prod_{f:n_f=1} \lambda_f \mu_f} \quad (2)$$

Thus, to derive the fraction of transmission time $T(f)$, it suffices to sum the steady-state probabilities of all states in the Markov chain M where flow f is active;

$$T(f) = \sum_{m \in M:m_f=1} \pi_m \quad (3)$$

Due to the reversibility of the Markov chain M [3], (2) is equally valid for different distributions of back-off times and transmission durations other than exponential (as long as their means are respectively $1/\lambda_f$ and μ_f for each flow f). Then, (3) is an accurate expression of the transmission time $T(f)$ in the networks with uniformly distributed back-off times and fixed packet lengths considered here (where we replace the mean transmission time μ_f by the fixed value d for each $f \in \mathcal{F}$).

Instead, the derivation of $S(f)$ represents a major challenge as several, possibly interdependent, factors can simultaneously affect a flow's success rate. For example, in this work we consider interference from transmitters in transmission range, interference from transmitters out of transmission range, and packet losses due to channel errors.

Given a set of factors $\{\phi_1, \dots, \phi_N\}$, denote as $c_y(f)$ the conditions required in the network for factor ϕ_y not to hinder the success of a transmission of f . Then, the probability $S(f)$ can be written as

$$\begin{aligned} S(f) &= \Pr(c_1(f), \dots, c_N(f)) \\ &= \Pr(c_1(f)) \times \Pr(c_2(f) \mid c_1(f)) \times \\ &\quad \dots \times \Pr(c_N(f) \mid c_{N-1}(f), \dots, c_1(f)) \end{aligned} \quad (4)$$

Equation (4) provides a general approach to break the interdependence of events in a CSMA wireless network where multiple factors simultaneously affect a flow's success rate. In contrast with the *numerical* iterative techniques used in [11]–[15], (4) combines the effects of all factors within a single step in a *product-form* expression. This is the key feature

⁴Note that, due to CS, no state in M has multiple neighbor transmitters active. However, in the case of hidden terminals, we do include states with transmitters out of transmission range of each other simultaneously active.

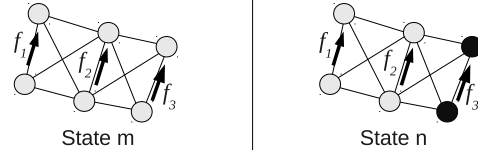


Fig. 3: Contention states for a flow f_1 in a 3-flow network. Dark node pairs represent active flows.

that enables the derivation of closed-form expressions, which would not be possible by the use of any numerical method.

For the factors considered here, (4) can be rewritten as

$$S(f) = S_r(f) \times S_{h|r}(f) \times S_{c|h,r}(f)$$

where, given an f 's transmission a , $S_r(f)$ is the probability that all interferers in transmission range of f are silent during a , $S_{h|r}(f)$ is the probability that all hidden interferers to f are silent during a given that all interferers in range of f are silent, and $S_{c|h,r}(f)$ is the probability that the transmission a does not fail due to channel errors given that during a all interferers to f are silent. In the following, we derive expressions for these conditional probabilities to be combined with (1) and (3) to form closed-form expressions of throughput.

C. Collisions with contending neighbors

To derive $S_r(\cdot)$, we need to account for simultaneous transmissions at interfering flows in transmission range. However, the set of neighbor nodes that can start simultaneous transmissions depends on the network state, as some of them may be deferring their transmissions due to CS. In the following, we present a method to derive $S_r(\cdot)$ determining the set of possible neighbor interferers separately for each network state.

For the transmitter u of a flow f to start transmitting, it must sense the channel idle. We call such a network state in which u and all its neighbors are silent, a *contention state* for f . Denote as $\bar{\mathcal{N}}(f)$ the set of states in the Markov chain M where all transmitters neighbor to u are silent, i.e.,

$$\bar{\mathcal{N}}(f) = \{m \in M / m_g = 0 \quad \forall g = (i, j) \in \mathcal{F} : (i, u) \in \mathcal{E}\}$$

Now, the set of contention states of flow f in the Markov chain M can be written as

$$\mathcal{C}(f) = \{m \in M / m \in \bar{\mathcal{N}}(f), m_f = 0\}$$

For example, Fig. 3 shows the contention states for a flow f_1 in a network with 3 flows. Given a state $m \in \mathcal{C}(f)$, the set of *interfering contender flows* of flow f in state m is

$$\mathcal{I}_r(f, m) = \{g \in \mathcal{I}_r(f) / m \in \bar{\mathcal{N}}(g)\}$$

For example, the sets of interfering contenders of flow f_1 in Fig. 3 are $\mathcal{I}_r(f_1, m) = \{f_2\}$ for state m , and $\mathcal{I}_r(f_1, n) = \emptyset$ for state n . Hence, the probability of collision for a transmission of f_1 starting on state n is zero (no contenders can start transmitting in the same time slot as f_1), whereas the probability

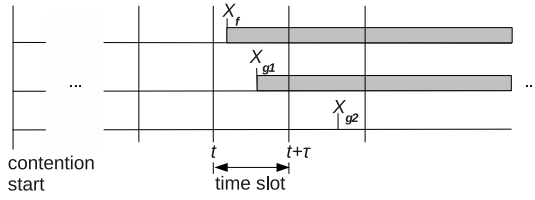


Fig. 4: A flow f contending against neighbor flows g_1 and g_2 . The exponentially-distributed back-off times are mapped to time slots dividing the timeline in periods of fixed length. In the example, the contending flow g_1 completes its back-off in the same time slot than f , but the flow g_2 does it after.

of collision for a transmission starting on state m depends on the aggressiveness of f_2 's transmitter.⁵

Then, we decompose the problem of deriving $S_r(f)$ by considering the conditional probability of each contention state for f . As *Poisson Arrivals See Time Averages* [4],

$$S_r(f) = \frac{\sum_{m \in \mathcal{C}(f)} \pi_m \times S_r(f, m)}{\sum_{n \in \mathcal{C}(f)} \pi_n} \quad (5)$$

where $S_r(f, m)$ is the probability that all interfering neighbors to f are silent during a transmission of f that started at the contending state m . In the example of Fig. 3, we have

$$S_r(f_1) = \frac{\pi_m}{\pi_m + \pi_n} S_r(f_1, m) + \frac{\pi_n}{\pi_m + \pi_n} \quad (6)$$

In the continuous-time CSMA model, the back-off time that flow f 's source waits before transmitting is the exponentially-distributed random variable $X_f \sim \text{Exp}(\lambda_f)$. Although such model provides accurate expressions of transmission time (as discussed before in Section II-B), it does not directly measure collisions of transmissions from neighbor nodes, as time slots are not readily incorporated. To overcome this, we first discretize the time as shown in Fig. 4, creating a mapping between exponential back-off times and time slots. Then, we derive $S_r(f, m)$ as the probability that no contending flows in $\mathcal{I}_r(f, m)$ complete its back-off in the same time slot than f ;

$$\begin{aligned} S_r(f, m) &= \Pr(t < X_f < \tau + t, X_g > \tau + t \quad \forall g \in \mathcal{I}_r(f, m) \mid \\ &\quad t < X_f < \tau + t, X_g > X_f \quad \forall g \in \mathcal{I}_r(f, m)) \\ &= \frac{\Pr(X_f < \tau, X_g > \tau \quad \forall g \in \mathcal{I}_r(f, m))}{\Pr(X_f < \tau, X_g > X_f \quad \forall g \in \mathcal{I}_r(f, m))} \end{aligned}$$

where τ is the duration of a time slot and t is the start of the slot where X_f lies.⁶

Integrating the joint exponential distribution for independent random variables over the corresponding time regions for numerator and denominator, we get

⁵While the network state can change *during* a flow's back-off procedure (for example, in Fig. 3 the two states m and n can alternate if the back-off time for flow f_1 is long enough), the memoryless property of the system allows us to focus on the very last contention state of a flow prior to its transmission, without keeping track of the previous system history.

⁶We know $X_f < X_g$ as these are the only cases that contribute to $T(f)$ in (3). Cases with $X_g < X_f$ are not counted as transmissions in the first place and should not be considered here.

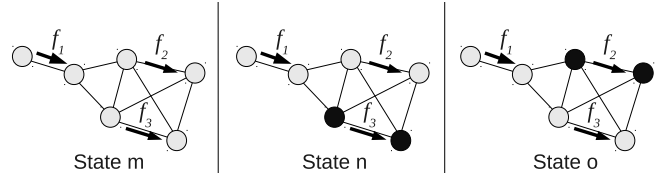


Fig. 5: Contention states for a flow f_1 in a 3-flow network with hidden interferers. Dark node pairs represent active flows.

$$S_r(f, m) = \frac{(\lambda_f + \sum_{g \in \mathcal{I}_r(f, m)} \lambda_g) (1 - e^{-\lambda_f \tau}) (e^{-\tau (\sum_{g \in \mathcal{I}_r(f, m)} \lambda_g)})}{\lambda_f (1 - e^{-\tau (\lambda_f + \sum_{g \in \mathcal{I}_r(f, m)} \lambda_g)}}$$

which can be substituted into (5) to derive the probability $S_r(f)$ over all contention states.

D. Collisions with hidden interferers

We now derive $S_{h|r}(f)$, the conditional probability that all hidden interferers to flow f are silent during a transmission of f for which all neighbor interferers are silent. Consider a transmission a of flow f . To avoid interference from hidden transmitters, two conditions must hold; (i) At the time a starts, no hidden interferers to f must be active, and; (ii) During the entire duration d of transmission a , no hidden interferer must start transmitting. Thus,

$$S_{h|r}(f) = S_{h|r}^\dagger(f) \times S_{h|r}^\ddagger(f)$$

where $S_{h|r}^\dagger(f)$ is the conditional probability that all hidden interferers to f are silent when f 's transmission starts (i.e., conditional on the fact that f is in a contention state), and $S_{h|r}^\ddagger(f)$ is the probability that no hidden interferers to f start transmitting for a period of time d given that at the beginning of such period all of them are silent (and that during the entire period d , f 's neighbors are silent as well).

Defining $\overline{\mathcal{H}}(f)$ as the set of states in the Markov chain M where all hidden interferers to f are silent (i.e., $\overline{\mathcal{H}}(f) = \{m \in M / m_g = 0 \quad \forall g \in \mathcal{I}_h(f)\}$), we have

$$S_{h|r}^\dagger(f) = \frac{\sum_{m \in (\overline{\mathcal{H}}(f) \cap \mathcal{C}(f))} \pi_m}{\sum_{n \in \mathcal{C}(f)} \pi_n}$$

For example, Fig. 5 shows all the contention states for a given flow f_1 in a 3-flow network. In that case,

$$S_{h|r}^\dagger(f_1) = \frac{\pi_m}{\pi_m + \pi_n + \pi_o} = \frac{1}{1 + d(\lambda_2 + \lambda_3)}$$

which decreases as the aggressiveness λ_2 and λ_3 of hidden interferers to access the channel increase.

To derive $S_{h|r}^\ddagger(f)$ note that, when f 's transmission starts, all hidden interferers are assumed to be silent (which is accounted for by $S_{h|r}^\dagger(f)$) and, during the entire transmission length d , all neighbor transmitters to f defer their transmissions. However, hidden interferers can start transmitting at some point during f 's transmission. To account for such an event,

we denote as Y_g^f the expected time-to-transmission of a flow $g \in \mathcal{I}_h(f)$ given that flow f is active, its neighbor flows are silent and all hidden interferers are initially silent. Assume that the transmission of flow f has just started. Then $S_{h|r}^\dagger(f)$ can be written as

$$\Pr(Y_g^f > d \quad \forall g \in \mathcal{I}_h(f)) = \Pr(\min_{g \in \mathcal{I}_h(f)} \{Y_g^f\} > d) \quad (7)$$

Because all hidden interferers are initially silent, up to the time $\min_{g \in \mathcal{I}_h(f)} \{Y_g^f\}$ they cannot influence each others' transmissions (a silent flow in a network has the same effect as if it was not present at all). Then, for the sake of deriving $\Pr(\min_{g \in \mathcal{I}_h(f)} \{Y_g^f\} > d)$ we can assume the times Y_g^f for all $g \in \mathcal{I}_h(f)$ to be independent random variables, and write

$$\Pr(\min_{g \in \mathcal{I}_h(f)} \{Y_g^f\} > d) = \prod_{\forall g \in \mathcal{I}_h(f)} \Pr(Y_g^f > d) \quad (8)$$

where each factor $\Pr(Y_g^f > d)$ can be derived separately assuming all hidden interferers other than g to be silent. Further, to simplify the derivation of $\Pr(Y_g^f > d)$, we assume that each variable Y_g^f follows an exponential distribution with parameter η_g^f , i.e., $Y_g^f \sim \text{Exp}(\eta_g^f) \quad \forall g \in \mathcal{I}_h(f)$. We call η_g^f the *transmission rate* of flow g given that all other hidden interferers and neighbors to f are silent. Then

$$\Pr(Y_g^f > d) = e^{-\eta_g^f \times d} \quad \forall g \in \mathcal{I}_h(f) \quad (9)$$

Finally, for each flow g we derive an expression of η_g^f . In order to do so, we first compute the fraction of transmission time T_g^f of g in a reduced network where we remove all flows neighbor to f and hidden interferers other than g (which is equivalent to silencing such flows).⁷ Then, using renewal arguments, it is easy to derive

$$\eta_g^f = \frac{T_g^f}{d - dT_g^f} \quad \forall g \in \mathcal{I}_h(f) \quad (10)$$

Combining (7), (8), (9), and (10), we obtain

$$S_{h|r}^\dagger(f) = \prod_{\forall g \in \mathcal{I}_h(f)} e^{-\frac{T_g^f}{1-T_g^f}}$$

where for each $g \in \mathcal{I}_h(f)$, T_g^f is the fraction of transmission time of g derived (using (3)) in a subnetwork of G where all flows neighbor to f and hidden interferers in $\mathcal{I}_h(f)$ except g have been removed.

For example, for the network in Fig. 5, we derive the expressions $T_{f_2}^{f_1} = \frac{d\lambda_2}{1+d\lambda_2}$ and $T_{f_3}^{f_1} = \frac{d\lambda_3}{1+d\lambda_3}$ as the transmission times $T(f_2)$ and $T(f_3)$ in subnetworks where the flows f_3 and f_2 have been removed, respectively. Then,

$$S_{h|r}^\dagger(f_1) = e^{-d\lambda_2} e^{-d\lambda_3} = e^{-d(\lambda_2+\lambda_3)}$$

which is indeed the probability that no transmissions at the flows f_2 and f_3 start for a time period of length d , since the sum of Poisson processes is yet another Poisson process with the sum of the rates.

⁷Flow f may also be removed, since after removing all neighbor flows its operation does not affect the transmission times in the rest of the network.

E. Closed-form throughput expressions

The analytical expressions derived in this section can be simplified by normalizing all time durations by d , and putting $R_f = \lambda_f d$, which we call the *normalized contention aggressiveness* of flow f . Then, by direct substitution in the expansion of (1), we obtain equivalent throughput equations that depend on the array parameter $\mathbf{R} \in \mathbb{R}^{|\mathcal{F}|}$, written as

$$\gamma_f(\mathbf{R}) = T(f, \mathbf{R}) \times S_r(f, \mathbf{R}) \times S_{h|r}(f, \mathbf{R}) \times S_{c|h,r}(f, \mathbf{R}) \quad (11)$$

A similar approach to the one described in the previous sections could be used to derive $S_{c|h,r}(f, \mathbf{R})$ as the conditional probability of no channel errors given that all interferers in $\mathcal{I}(f)$ are silent, by accounting for transmissions of flows that are too distant from f to interfere with it (i.e., flows out of $\mathcal{I}(f)$), yet can contribute to raise the noise level at the receiver.

However, in scenarios where the main contribution to channel errors is due to environmental noise and external factors, good results can be obtained assuming channel errors to be independent from MAC protocol operation. In that case, we set $S_{c|h,r}(f, \mathbf{R}) = e_f$, where $e_f \in [0, 1]$ is the complement of the average packet loss rate of f 's channel in isolation. We use this second approach for the model validation, measuring packet loss rates directly from our wireless testbed platform.

III. SIMULATIONS AND EXPERIMENTAL VALIDATION

A. Model implementation and validation setup

Traditional model implementations return the value of model functions at specific points in their domain by means of *numerical* computations. In contrast, to leverage the full potential of closed-form expressions, we developed a *symbolic* model implementation, which inputs a network topology and outputs the throughput expressions specified by (11) as equations where model parameters such as \mathbf{R} appear as variables. This enables algebraic manipulation of the returned throughput expressions for any analytical purpose. For example, the generated expressions are compatible with Matlab, can be plotted in Gnuplot as continuous functions or embedded into scripts or application source code for further processing.

We validate our analytical model using realistic simulations and experiments with real wireless hardware. Our simulator is based on the 802.11 implementation of NS-2, with minor extensions to enable the assignment of arbitrary CW sizes to each node (thus allowing a *complete* model evaluation, not limited to specific CW sizes, such as integer powers of 2).

For our experiments with real wireless hardware, we run the CSMA implementation in [20] on the WARP platform,⁸ whose open design provides complete access to all events of interest at PHY and MAC layers. For each experiment, we deploy an indoor wireless network testbed of WARP nodes, setting the required topology by adjusting the transmission power levels and the relative position of nodes within the environment. Fig. 6 shows the wireless testbed components.

⁸<http://warp.rice.edu>

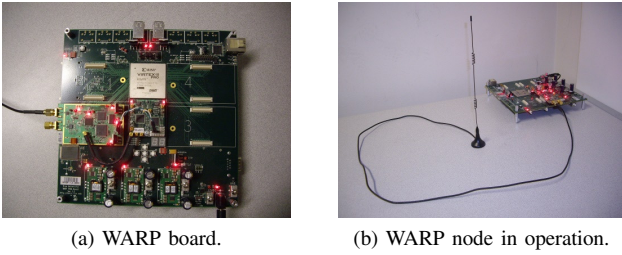


Fig. 6: Wireless testbed components.

	Experiments	Simulations
Time slot duration	0.022ms	0.02ms
Header+PLCP duration	0.135ms	0.192ms
DATA duration	2.61ms	4.216ms
DATA payload	8000bits	8000bits
SIFS	0.014ms	0.01ms
ACK duration	0.125ms	0.304ms
DIFS	0.06ms	0.05ms
EIFS	0.24ms	0.364ms

TABLE I: System parameters.

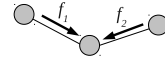
In both simulator and wireless testbed, data transmissions are subject to overhead such as headers, inter-frame spaces, and ACK control packets sent over the reverse link. To account for them, we add their duration as part of the transmission length d in the analytical model. Then, we obtain the average throughput received by a flow f from the fraction of successful transmission time as $\gamma_f(\mathbf{R}) \times \frac{\theta}{d}$, where θ is the payload size of a data packet measured in bits. Table I summarizes the system parameters used for validation.

B. Experimental validation over selected topologies

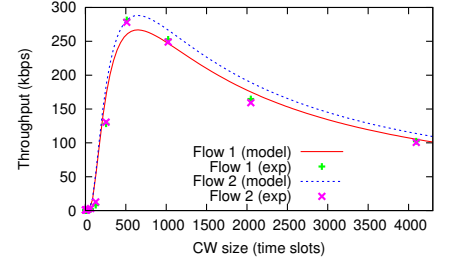
We conducted an extensive experimental validation to evaluate the accuracy of our model. In this section we show selected results in scenarios known to be critical in determining the network-wide throughput distribution [10], [14].

For example, in topologies with *hidden terminals*, like the one in Fig. 7a, packet collisions have a relatively high probability due to the inability of transmitters to carrier-sense each other. While the probability of collision can be reduced to arbitrarily low values by setting large-enough CW sizes, excessively long CWs can lead to channel underutilization, thereby decreasing throughput. Our testbed experiments show that the model accurately accounts for these two factors via the expressions $S_{h|r}(\cdot)$ and $T(\cdot)$, respectively. As a result, it closely matches the flow throughput measured in the WARP testbed (see Fig. 7b), with an error normalized over the channel capacity of about 0.5% averaged over all evaluated data points. The small difference in the model-predicted throughput between the two flows is due to the difference in the channel error rates measured for each link and accounted in $S_{c|h,r}(\cdot)$.

In the previous example, the two flows are subject to a *symmetric* interference relation. However, a common scenario arising in practice is when one flow interferes with the other, but not vice versa. An example of such a scenario with *asymmetric* interference is depicted in Fig. 8a. In this network, termed *information asymmetry* in [10], the uneven probability of collision at flow receivers can lead to large throughput dis-

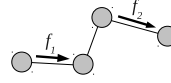


(a) Network topology.

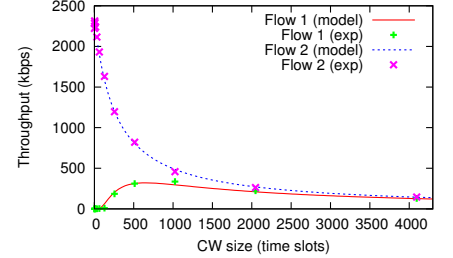


(b) Flow throughput as a function of CW size.

Fig. 7: Model validation in a topology with hidden terminals.



(a) Network topology.



(b) Flow throughput as a function of CW size.

Fig. 8: Model validation in a topology with information asymmetry.

parities or even the total starvation of flow f_1 . However, thanks to the general definition of $\mathcal{I}_h(f)$, which admits asymmetric interference relations, our model captures the asymmetries in the network and returns a different expression of $S_{h|r}(\cdot)$ for each flow. This yields very accurate results, closely matching the actual flow throughput in our experiments, with an error normalized over the channel capacity and averaged over all evaluated data points less than 1% (Fig. 8b).

Finally, the inability of hidden nodes to carrier-sense each other can also introduce problems of coordination among flows, such as in the topology with a *flow-in-the-middle*, depicted in Fig. 9a. In this network, the side flows f_1 and f_3 can successfully transmit simultaneously, while the central flow f_2 can only access the channel when the two side flows are silent. Furthermore, transmissions at the two side flows may repeatedly overlap in time leaving no idle time for the central flow to transmit, which in some cases can lead to the starvation of the central flow [14], [19].

As observed in Fig. 9b, the model accurately determines flow throughput closely matching experimental results. This is due to both; (i) the accuracy of $T(\cdot)$ measuring the fraction of flow transmission time, thereby capturing the situations where side flows monopolize the use of the channel, and; (ii) the selective feature of $S_r(\cdot)$ weighting contention states according to their probabilities. For example, with short CW values, collisions between f_1 and f_2 are unlikely to occur, as the high activity of flow f_3 prevents f_2 from transmitting. This situation is captured by (6), which weights the idle state m with a very low probability. As a consequence, the model closely matches experimental results, with less than 2% average error

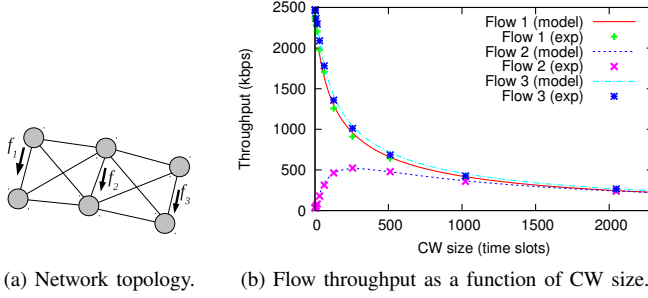


Fig. 9: Model validation in a topology with a flow-in-the-middle.

normalized over the channel capacity.

C. Complex scenarios with multiple interference constraints

We extend the model validation to more complex scenarios where several factors simultaneously affect the throughput distribution in different ways. To this end, we consider two wireless networks representative of different networking scenarios; (i) a *sparse* network with 7 flows generated on a $1000\text{m} \times 1000\text{m}$ area, and; (ii) a *denser* network with 10 flows generated on a $500\text{m} \times 500\text{m}$ area.⁹ We use these two networks, respectively depicted in Fig. 10 and 12, to evaluate the accuracy of the model by means of realistic simulations.

1) **A 7-flow sparse network:** The network depicted in Fig. 10 contains a mixture of the previously discussed problematic scenarios, such as *hidden terminals* (e.g., flows 1 and 4), *information asymmetry* (e.g., flows 3 and 4), and *flow-in-the-middle* (e.g., flows 5, 3, and 6),¹⁰ as well as *fully-connected* groups (e.g., flows 1 and 2) and non-conflicting flow pairs (e.g., flows 1 and 7).

We analyze the variations of flow throughput for multiple network-wise symmetric CW assignments, depicted in Fig. 11. We identify subsets of flows that, given their similar situation, share a common trend in the attained throughput. Flows 6 and 7 are privileged, dominating over flow 5 in information asymmetry and as side flows to flow 3 in a flow-in-the-middle relation. As a result, flows 6 and 7 attain high throughput in all cases except for very short CWs (about 7 slots or less), which increases their probability of mutual collision. Flows 1 and 2 form a fully-connected group, yet they suffer interference from the hidden flow 4. Thus, their throughput is lowered by a higher collision probability, and can only attain moderate values when the CW size is large enough (from about 1000 to 2000 slots). Finally, flows 3, 4, and 5 are the most disadvantaged, hindered by multiple other flows simultaneously in either hidden terminals, information asymmetry and flow-in-the-middle relationships. The throughput of these

⁹While even denser networks are also possible (e.g., fully-connected networks), very dense networks with most nodes in transmission range of each other are easier to model and present less challenging problems to the operation of CSMA, since hidden terminals and related factors become less frequent as the degree of node connectivity raises.

¹⁰Although flow 5's transmissions can collide with node 6's transmissions, the effect of CW sizes on the central flow 3 in terms of sensed busy time are the same as in the previously discussed flow-in-the-middle scenario.

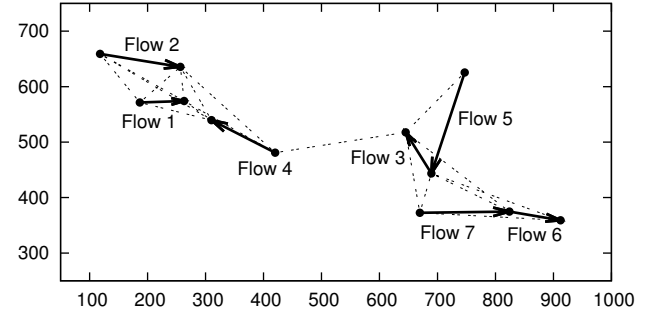


Fig. 10: A sparse 7-flow wireless network with multiple interference relations among flows.

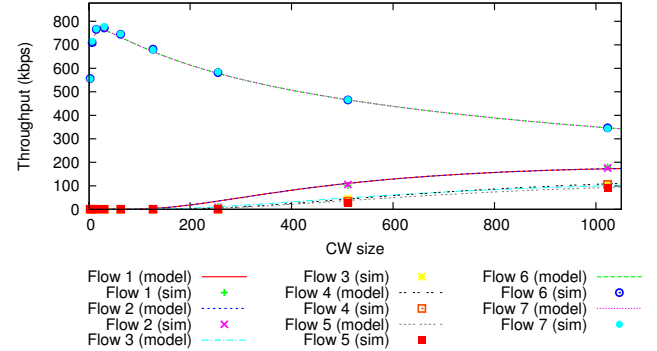


Fig. 11: Flow throughput as a function of CW size in the 7-flow network of Fig. 10, for both model and simulation results.

flows is poor for any symmetric CW assignment. Regardless of the factors involved, the model accurately tracks variations in the throughput due to CW sizes, with a normalized error less than 0.5% on average over all evaluated points.

2) **A 10-flow network with higher node density:** We now consider the network depicted in Fig. 12. As in the previous case, the 10-flow network comprises a mixture of *hidden terminals* (e.g., flows 6 and 10), *information asymmetry* (e.g., flows 8 and 10), *flow-in-the-middle* (e.g., flows 1, 5 and 8), non-conflicting node pairs (e.g., flows 7 and 8), and *fully-connected* groups (e.g., flows 2 and 9).

Fig. 13 compares the model-predicted throughput against the actual flow throughput measured from the simulations, for multiple network-wise CW assignments. The most advantaged flows, such as flows 1, 2, 7 and 8, have all interfering flows in transmission range, and only suffer high collisions for very small CW sizes. Hence, these flows attain significantly more throughput than the others. Furthermore, such flows are located on the sides of the network, and monopolize the use of the channel over the central flows 3, 4, 5, 9 and 10, due to the same coordination problems than in the flow-in-the-middle topology. Finally, high collisions due to hidden terminals and information asymmetry drastically reduce the throughput of specific flows, such as 6 and 10.

Again, regardless of the factors involved, the model accurately tracks variations in the throughput due to CW sizes, with a normalized error less than 0.6% on average over all evaluated

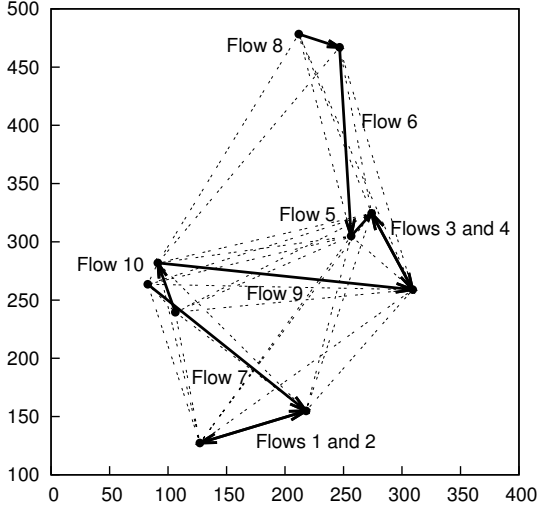


Fig. 12: A 10-flow wireless network with multiple interference relations among flows.

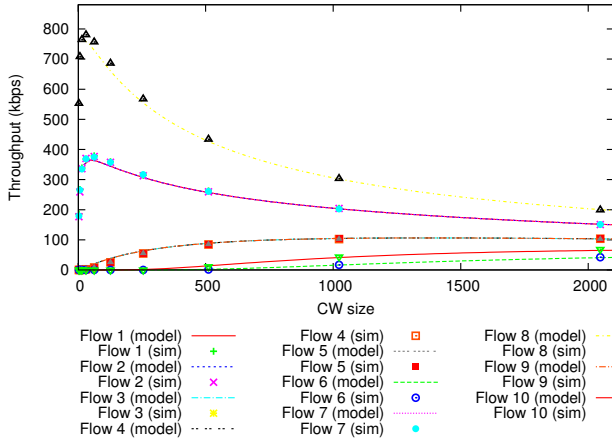


Fig. 13: Flow throughput as a function of CW size in the 10-flow network of Fig. 12, for both model and simulation results.

points. This comprises collisions in transmission range, hidden terminals, information asymmetry, flow-in-the-middle, and combinations of multiple factors manifesting simultaneously.

IV. APPLICATION EXAMPLE: NETWORK UTILITY MAXIMIZATION

A. Hidden terminals

The problem of optimizing utility in networks *without hidden terminals* is greatly simplified by the fact that the capacity area of such networks is convex [21], which allows to derive gradient-descent methods that can be mapped to distributed operations in the network under certain assumptions [21], [22].

With hidden terminals, instead, the capacity area of CSMA networks cannot be assumed to be convex. For example, consider the network topology depicted in Fig. 7a. Using (11), the throughput expressions for the two flows f_1 and f_2 in the network are, respectively;

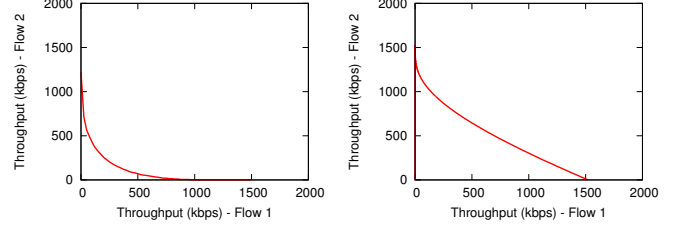


Fig. 14: Capacity region of networks with hidden interferers. System parameters are those for simulations in Table I.

$$\gamma_{f_1}(\mathbf{R}) = \frac{R_1}{1 + R_1} \frac{1}{1 + R_2} e^{-R_2 c}$$

and

$$\gamma_{f_2}(\mathbf{R}) = \frac{R_2}{1 + R_2} \frac{1}{1 + R_1} e^{-R_1 c}$$

where c is a constant that depends on the ratio between payload size and transmission duration (θ/d). Using such expressions, we plot the capacity area C of the network (see Fig. 14a). It is easy to see that such area is non-convex; in fact, both points $(1000, 0)$ and $(0, 1000)$ are in C , but their convex combination $(500, 500) = \frac{1}{2}(1000, 0) + \frac{1}{2}(0, 1000)$ is outside of C .

While the derivation of distributed algorithms for network utility maximization is far beyond the scope of this work, we show that (11) can be used to determine the best CW assignments among nodes in a network combining hidden terminals, topological asymmetries, flow-in-the-middle and transmitters in transmission range of each other. The joint effect of all such critical factors is not captured by prior models for CSMA wireless network optimization.

Considering a logarithmic utility function of throughput $U_f(\mathbf{R}) = \log(\gamma_f(\mathbf{R}))$, the network utility is given by

$$U(\mathbf{R}) = \sum_{f \in \mathcal{F}} U_f(\mathbf{R}) = \sum_{f \in \mathcal{F}} \log(\gamma_f(\mathbf{R})) \quad (12)$$

Maximizing this function is known to yield an optimal *proportional fair* throughput distribution in the network;¹¹

$$\mathbf{R}^* = \underset{\mathbf{R} \in (\mathbb{R}_{\geq 0}^{|\mathcal{F}|})}{\text{arg_max}} \left\{ \sum_{f \in \mathcal{F}} \log(\gamma_f(\mathbf{R})) \right\}$$

For the hidden terminal scenario considered here, differentiating (12) with respect to R_1 and R_2 and equating to zero yields the optimal assignment $R_1^* = R_2^* = (\sqrt{2} - 1) \simeq 0.4142$, which corresponds to a CW of 1154 slots at each transmitter.¹²

¹¹While we focus on logarithmic utility optimization for illustrative purposes, the analysis presented here easily extends to maximizing other functions of throughput, such as total network throughput or alternative fairness measures. For example, it can be seen from Fig. 14a that maximum network throughput can be attained by silencing one of the transmitters and assigning all capacity to the other one.

¹²We further verify that the point $((\sqrt{2} - 1), (\sqrt{2} - 1))$ satisfies the second order conditions to be a maximum, which we omit here for brevity.

B. Asymmetric interference

The previous example refers to a scenario with hidden transmitters and *symmetric* interference. However, as anticipated in Section III-B, topological relations among nodes can lead to *asymmetric* interference, which in turn can yield extreme throughput disparities among flows. In this section, we illustrate the maximization of utility under asymmetric interference constraints using the network in Fig. 8a.

In this network, the throughput expression (11) for the two flows f_1 and f_2 respectively reduces to

$$\gamma_{f_1}(\mathbf{R}) = \frac{R_1}{1 + R_1} \frac{1}{1 + R_2} e^{-R_2 c}$$

and

$$\gamma_{f_2}(\mathbf{R}) = \frac{R_2}{1 + R_2} c$$

Similar to the previous case, the capacity area of the network with asymmetric interference is non-convex, as depicted in Fig. 14b. Differentiating the network utility function $U(\mathbf{R}) = \log(\gamma_{f_1}(\mathbf{R})) + \log(\gamma_{f_2}(\mathbf{R}))$ and equating to zero yields the following system of equations;

$$\begin{cases} \frac{dU(\mathbf{R})}{dR_1} = \frac{1}{R_1^2 + R_1} = 0 \\ \frac{dU(\mathbf{R})}{dR_2} = \frac{1}{R_2} - \frac{2}{R_2 + 1} - 1 = 0 \end{cases}$$

While $\frac{dU(\mathbf{R})}{dR_2} = 0$ can be satisfied by choosing $R_2^* = (\sqrt{2} - 1) \simeq 0.4142$, the equation $\frac{dU(\mathbf{R})}{dR_1} = 0$ admits no solution in $\mathbb{R}_{>0}$. However, note that $\frac{dU(\mathbf{R})}{dR_1}$ is a positive, decreasing function of R_1 over the whole set $\mathbb{R}_{>0}$. Thus, for any fixed value of R_2 , the function $U(\mathbf{R})$ is an upper-bounded, concave monotonically increasing function of R_1 . Therefore, the function $U(R_1, R_2^*)$ asymptotically reaches its maximum value as $R_1 \rightarrow +\infty$. In other words, to maximize network utility in the considered topology with asymmetric interference, flow f_1 should access the medium as aggressively as possible (i.e., using a CW of zero length), whereas flow f_2 should use the moderate aggressiveness $R_2^* = (\sqrt{2} - 1)$, which translates to a CW of 1154 slots.

C. Utility maximization on larger CSMA networks

We extend the example of network utility maximization to larger networks with multiple interference constraints. To this end, we use the 7-flow network depicted in Fig. 10 and the 10-flow network depicted in Fig. 12, which represent different networking scenarios (respectively, a *sparse* network and a network with *higher node density*). As previously discussed, such networks contain a mixture of problematic scenarios, including *hidden terminals*, *information asymmetry*, and *flow-in-the-middle*, as well as *fully-connected* groups and non-conflicting flow pairs.

In the previous examples, the small number of nodes leads to a small system of equations mathematically tractable for direct derivation of optimal points. Instead, in the complex scenarios of Fig. 10 and 12, the larger system of long, non-linear equations makes it impractical to maximize utility

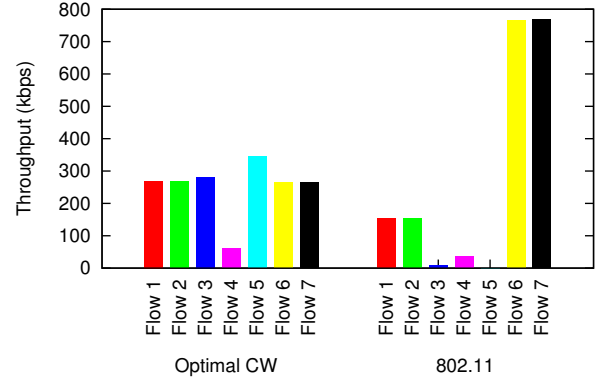


Fig. 15: Comparison between the per-flow throughput distribution of CSMA with optimal CW assignments and 802.11, in the 7-flow network of Fig. 10.

following the same approach. Furthermore, a numerical search over the set of possible CW assignments remains unfeasible even when restricting it to a few possible values per node, as the search space grows exponentially with the number of flows.¹³

Instead, we leverage the advantages of our model symbolic implementation by plugging our throughput expressions within Matlab's Global Optimization Toolbox. Then, for each scenario, we run a global search based on multiple executions of the gradient descent method `fmincon`, in case the objective utility function presents more than one local maximum point. Finally, we use the best solution to determine per-node CW assignments that maximize network utility.

1) **The 7-flow sparse network:** For the network in Fig. 10, we start the gradient descent method at 5000 different points, obtaining the same solution in all cases. Fig. 15 shows the throughput distribution in such a scenario with the derived optimal CW assignments compared to the throughput distribution of 802.11 with BEB. We note that the optimal CW assignment significantly reduces throughput disparities, increasing the throughput of flows 1 to 5 and bringing flows 3 and 5 out of the starvation situation. This results in a 22% increase of network utility, with an average per-flow throughput gain of about 550% (ignoring flow 5 whose percentage gain is infinite).

We now illustrate the accuracy of the derived optimal point by the use of extensive simulations. In this case, we drastically reduce the number of required simulations in two ways; first, we reduce the set of possible CW assignments to a small set in close proximity to the already-determined optimal point CW^* . Second, we only vary one element of CW^* at a time, keeping the others fixed to the optimal, measuring the variations of $U(\cdot)$ over each orthogonal axis. This way, the required number of simulations grows only linearly with the number of network flows. Fig. 16 shows the obtained results. Although this does not constitute a rigorous proof of correctness, we do observe

¹³For example, restricting the possible CW assignments to only 10 different values in our 7-flow scenario would lead to a search space as large as 10^7 possible network-wise assignments.

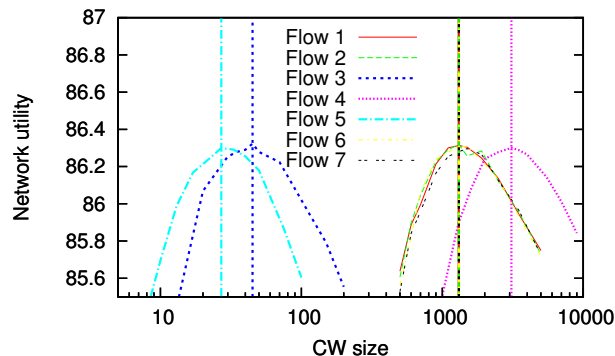


Fig. 16: Network utility as a function of CW size along each orthogonal axis, for the 7-flow network topology in Fig. 10. Curves in the plot interpolate data points obtained by simulation, whereas vertical lines indicate optimal point coordinates derived by the optimization method.

a strong trend for the network utility to decrease in all the considered directions as the distance to the optimal point CW^* increases.

2) **The denser 10-flow network:** For the network in Fig. 12, we run 5000 gradient descent executions from distinct starting points, obtaining the same solution in all cases. Fig. 17 shows the throughput distribution in such a scenario with the derived optimal CW assignments compared to the throughput distribution of 802.11 with BEB. With 802.11, flows 1, 2, 7 and 8 dominate over other flows in flow-in-the-middle and information asymmetry relations. Also flow 6 is a side flow dominating over central ones, but its throughput is hindered by high collisions with flows 1 and 2 at its receiver. As a consequence, central flows starve, whereas dominant side flows 1, 2, 7 and 8 receive high network throughput.

In contrast, the optimization method assigns large CW sizes to all dominant flows, reducing their aggressiveness in the contention for the channel and significantly increasing the number of transmission opportunities for the central flows. This results in a throughput increase at all central flows, for which the starvation problem is solved. Furthermore, the network utility is increased of 37%, with an average per-flow throughput gain of about 3100% (ignoring flows 5 and 9 whose percentage gain is infinite).

Finally, we illustrate the accuracy of the derived optimal point using the same method as for the 7-flow network. Fig. 18 shows the variations of actual network utility over each orthogonal axis for different CW assignments, obtained by simulation. Again, we observe a strong trend for the network utility to decrease in all the considered directions as the distance to the optimal point CW^* increases.

V. RELATED WORK

Research in wireless CSMA throughput models started with analysis of fully-connected networks, e.g., [1], which derived throughput as a function of the offered load. More recently, [6] presented a throughput analysis based on a Markov chain model that incorporates aspects specific to the IEEE 802.11

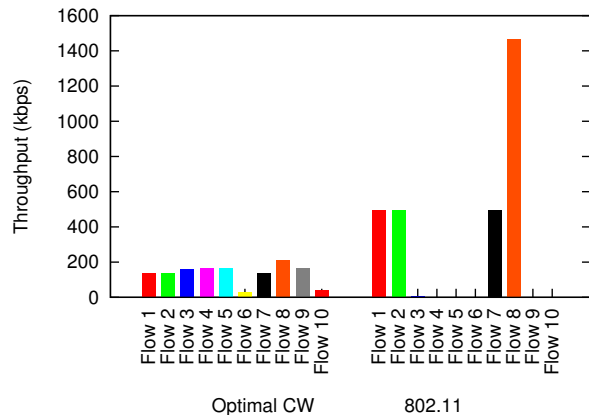


Fig. 17: Comparison between the per-flow throughput distribution of CSMA with optimal CW assignments and 802.11, in the 10-flow network of Fig. 12.

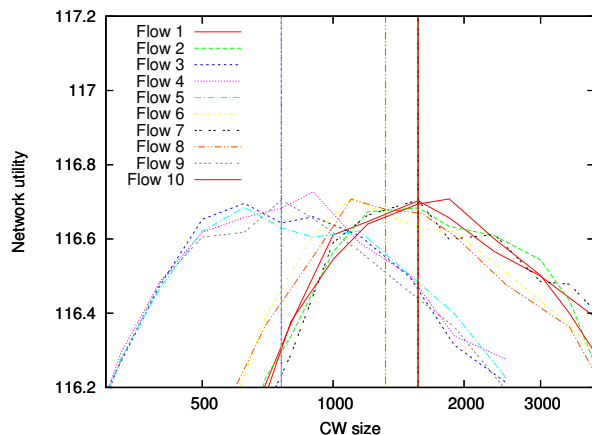


Fig. 18: Network utility as a function of CW size along each orthogonal axis, for the 10-flow network topology in Fig. 12. Curves in the plot interpolate data points obtained by simulation, whereas vertical lines indicate optimal point coordinates derived by the optimization method.

protocol. Although these works are specific to fully-connected networks, they provide important contributions to understand the relation between system parameters and CSMA capacity.

Other work considers more general topologies with hidden terminals, [2], [7]–[9], [11]–[15]. Each of these is based on a different set of assumptions and modeling techniques, which makes them suitable for different purposes. Using a *node-centric* approach, [8] provides a lower bound of flow throughput whose accuracy depends on the fraction of hidden terminals in the network. [2] derives elegant product-form expressions under a perfect capture model. [9] instead assumes perfect RTS/CTS messages that are always successful in reserving a free channel. [7] presents a physical-interference model that realistically models interference effects at the physical layer, assuming complete overlap of all simultaneous transmissions. Finally, [11]–[15] are based on a decoupling technique, which divides the network into specific scenarios of

easier analysis. An iterative procedure is then used to combine the results obtained for such atomic scenarios in order to determine per-flow throughput at the network scale.

Unfortunately, the above methods may not be suitable for the analysis of some scenarios presented here. For example, starvation in the information asymmetry topology is not characterized under perfect capture, and manifests even with the use of RTS/CTS mechanisms [16]–[18]. Similarly, partial overlapping is a determinant factor leading to throughput disparities in topologies with a flow-in-the-middle [19], a behavior not characterized by [7]. Finally, the iterative procedure in [11]–[15] requires numerical computations, and does not provide closed-form expressions for throughput analysis.

While multiple factors can simultaneously affect flow throughput in CSMA wireless networks, our method is general enough to capture the three main factors in [10], [14] that have been proven critical in determining throughput distributions at the network scale; namely hidden terminals, information asymmetry and flow-in-the-middle. Furthermore, it characterizes flow throughput in CSMA networks using a single equation, without the use of iterative or aggregation procedures. Unlike most previous work, we use experiments in addition to simulations to evaluate the accuracy of our models.

VI. CONCLUSION

We presented closed-form expressions of throughput for CSMA wireless networks with collisions and hidden terminals. The key modeling principle driving our approach is to break the interdependence of events in a wireless network by the use of conditional expressions. Our experimental validation shows that the model features play an essential role characterizing CSMA performance, and accurately capture combinations of the main critical factors determining throughput distribution at the network scale. Furthermore, we have shown how the model enables unprecedented network studies through a concrete example of utility maximization in complex networks with a combination of collisions, hidden terminals, asymmetric interference and flow-in-the-middle (which were not jointly addressed to date by other models for wireless CSMA optimization), yielding excellent results.

REFERENCES

- [1] L. Kleinrock and F. A. Tobagi, "Packet switching in radio channels: Part I - Carrier Sense Multiple-Access modes and their throughput-delay characteristics," *IEEE Trans. on Communications*, Vol. COM-23, No. 12, pp. 1400-1416, Dec. 1975.
- [2] R. R. Boorstyn, A. Kershenbaum, B. Maglaris, and V. Sahin, "Throughput analysis in multihop CSMA packet radio networks," *IEEE Trans. on Communications*, Vol. COM-35, No. 3, pp. 267-274, March 1987.
- [3] F. Kelly, "Reversibility and Stochastic Networks," Wiley, Chichester, 1979.
- [4] R. W. Wolff, "Poisson Arrivals See Time Averages," *Operations Research*, Vol. 30, No. 2, March-April 1982.
- [5] F. Kelly, "Stochastic models of computer communication systems," *Journal of the Royal Statistical Society*, Vol. 47, No. 3, pp. 379-395, 1985.
- [6] G. Bianchi, "Performance analysis of the IEEE 802.11 distributed coordination function," *IEEE Journal on Selected Areas in Communications*, Vol. 18, No. 3, pp. 535-547, March 2000.
- [7] M. M. Carvalho and J. J. Garcia-Luna-Aceves, "A scalable model for channel access protocols in multihop ad hoc networks," in *Proc. of ACM MobiCom*, Philadelphia, PA, Sept. 2004.
- [8] H. S. Chhaya and S. Gupta, "Performance modeling of asynchronous data transfer methods of IEEE 802.11 MAC protocol," *ACM Wireless Networks*, Vol. 3, No. 3, pp. 217-234, 1997.
- [9] X. Wang and K. Kar, "Throughput modelling and fairness issues in CSMA/CA based ad hoc networks," in *Proc. of IEEE INFOCOM*, Miami, FL, 2005.
- [10] M. Garetto, J. Shi, and E. W. Knightly, "Modeling media access in embedded two-flow topologies of multihop wireless networks," in *Proc. of ACM MobiCom*, Cologne, Germany, Sept. 2005.
- [11] K. Medepalli and F. A. Tobagi, "Towards performance modeling of IEEE 802.11 based wireless networks: A unified framework and its applications," in *Proc. of IEEE INFOCOM*, 2006.
- [12] Y. Gao, D. Chiu, and J. C. S. Lui, "Determining the end-to-end throughput capacity in multi-hop networks: Methodology and applications," in *Proc. ACM Sigmetrics*, pp. 39-50, June 2006.
- [13] L. Qiu, Y. Zhang, F. Wang, M. K. Han, and R. Mahajan, "A general model of wireless interference," in *Proc. of ACM MobiCom*, Montréal, Québec, Canada, Sept. 2007.
- [14] M. Garetto, T. Salonidis, and E. W. Knightly, "Modeling per-flow throughput and capturing starvation in CSMA multihop wireless networks," *IEEE/ACM Trans. on Networking*, Vol. 16, No. 4, pp. 864-877, Aug. 2008.
- [15] A. Jindal and K. Psounis, "The achievable rate region of 802.11-scheduled multihop networks," *IEEE/ACM Trans. on Networking*, Vol. 17, No. 4, Aug. 2009.
- [16] J. Camp, E. Aryafar, and E. W. Knightly, "Coupled 802.11 flows in urban channels: Model and experimental evaluation," in *Proc. of IEEE INFOCOM*, San Diego, CA, March 2010.
- [17] V. Bharghavan, A. Demers, S. Shenker, and L. Zhang, "MACAW: A media access protocol for wireless LANs," in *Proc. of ACM SIGCOMM*, London, UK, 1994.
- [18] V. Kanodia, C. Li, A. Sabharwal, B. Sadeghi, and E. W. Knightly, "Ordered packet scheduling in wireless ad hoc networks: Mechanisms and performance analysis," in *Proc. of ACM MobiHoc*, Lausanne, Switzerland, June 2002.
- [19] C. Chaudet, I. Guérin Lassous, E. Thierry, and B. Gaujal, "Study of the impact of asymmetry and carrier sense mechanism in IEEE 802.11 multi-hop networks through a basic case," in *Proc. of PE-WASUN'04*, Venice, Italy, Oct. 2004.
- [20] "CSMA MAC - WARP OFDM Reference Design v16.1", available at <http://warp.rice.edu/trac/wiki/OFDMReferenceDesign/Changelog>
- [21] L. Jiang and J. Walrand, "A distributed CSMA algorithm for throughput and utility maximization in wireless networks," in *Proc. of the Allerton Conference*, Monticello, IL, 2008.
- [22] J. Liu, Y. Yi, A. Proutiere, M. Chiang, and H. V. Poor, "Towards utility-optimal random access without message passing," *Wiley Journal of Wireless Communications and Mobile Computing*, vol. 10, no. 1, pp. 115-128, Jan. 2010.